

Immunohistochemical detection of angiotensin II receptors in mouse cerebellum and adrenal gland using “in vivo cryotechnique”

Zheng Huang · Nobuhiko Ohno · Nobuo Terada ·
Yurika Saitoh · Jiaorong Chen · Shinichi Ohno

Accepted: 12 February 2013 / Published online: 21 March 2013
© Springer-Verlag Berlin Heidelberg 2013

Abstract Angiotensin II (AT) receptors, including AT receptor type 1 (AT1R) and type 2 (AT2R), are expressed in the rodent central nervous system, but their distributions and activation states are still unclear. In this study, we have performed immunohistochemical analyses of AT receptors in mouse cerebellum and adrenal gland using our “in vivo cryotechnique” (IVCT). We used antibodies against amino-terminal domains of AT receptors, which are considered to undergo conformational changes upon the binding of AT. Immunoreactivity of AT1R was detected in mouse cerebellum, and was highest in the outer tissue areas of molecular layers using IVCT. The AT1R immunostaining largely overlapped with glial fibrillary acidic protein (GFAP), a marker of Bergmann glia. Surprisingly, the AT1R immunoreactivity in the cerebellar cortex was remarkably reduced following 5 and 10 min of hypoxia or direct administration of an AT1R antagonist, losartan. By contrast, in the adrenal cortex, such AT1R immunoreactivity detected at the zona glomerulosa did not change even after 15 min of hypoxia. The correlation of localization with GFAP and also hypoxia-induced decrease of its immunoreactivity were similarly observed by immunostaining of AT2R in the cerebellar specimens. These findings demonstrated that IVCT is useful to reveal dynamically changing immunoreactivities usually affected by receptor-ligand binding as well as hypoxia, and also suggested that functional activities of AT receptors are

time-dependently modulated under hypoxia in the central nervous system in comparison with the adrenal glands.

Keywords In vivo cryotechnique · Angiotensin II receptors · Cerebellum · Bergmann glia · Hypoxia

Introduction

Angiotensin II receptors, type 1 (AT1R) and type 2 (AT2R), belong to the superfamily of seven-transmembrane G-protein-coupled receptors (Gasparo et al. 2000), and mediate the physiological functions of angiotensin II (AT), an octapeptide hormone regulating cardiovascular homeostasis, in various organs of animals (Basso and Terragno 2001). Both AT1R and AT2R usually localize in the zona glomerulosa of adrenal cortical tissues, and AT-binding to the receptors mediates intracellular synthesis and secretion of aldosterone hormone in the well-known renin–angiotensin–aldosterone system (Frei et al. 2001; Harada et al. 2010). Some previous studies also demonstrated that AT receptors were often expressed in neurons and glia of the central nervous system (CNS), and play some functional roles in hemodynamic control, differentiation, neuronal plasticity and cell survival (Changaris et al. 1978; Saavedra 1992; Phillips et al. 1993; Allen et al. 1998; Fogarty and Matute 2001). Although both AT1R and AT2R are expressed in animal cerebellum (Reagan et al. 1994; Jöhren et al. 1998; Cote et al. 1999; Arce et al. 2001; Arce et al. 2011), their distributions and activation states under physiological and pathological conditions have not been well understood.

In the last one and a half decades, our “in vivo cryotechnique” (IVCT) has become well known as a powerful tool to retain native ultrastructures in brain

Z. Huang · N. Ohno · N. Terada · Y. Saitoh · J. Chen ·
S. Ohno (✉)

Department of Anatomy and Molecular Histology,
Interdisciplinary Graduate School of Medicine and Engineering,
University of Yamanashi, 1110 Shimokato, Chuo-city,
Yamanashi 409-3898, Japan
e-mail: sohno@yamanashi.ac.jp

tissue sections, such as extracellular spaces in mouse cerebellar cortex (Ohno et al. 2007, 2010). In addition, using IVCT followed by freeze-substitution (FS) fixation, unstable signal molecular components in animal organs were instantly captured in situ and could be immunohistochemically visualized without technical artifacts due to anoxia and ischemia (Terada et al. 2006). Therefore, the functional activities of AT receptors could be examined using IVCT along with specific antibodies, whose immunoreactivities usually depend on the dynamic binding of ligands and agonists to the receptors (Gupta et al. 2007). G-Protein-coupled receptors, including AT1R and AT2R, undergo rapid conformational changes of extracellular amino-terminal regions upon the binding of AT ligands and agonists (Fadhil et al. 2004). Therefore, some immunoreactivity changes of specific antibodies against the amino-terminal regions of such receptors could reflect alterations of ligand-binding activities and rapid adaptation for the intracellular metabolism and microenvironment.

In the present study, we used the IVCT and also antibodies against amino-terminal regions of AT receptors, and performed immunohistochemical analyses of mouse cerebellum in comparison to the common adrenal glands, where both localizations and functions of AT receptors have been well studied. We also examined their immunoreactivity changes under normal or hypoxic conditions using IVCT. Our present results demonstrated that immunoreactivities of dynamically changing AT1R and AT2R were clearly detected using IVCT, and were closely related to Bergmann glia and some astrocytes immunopositive for glial fibrillary acidic protein (GFAP). In addition, the AT1R immunoreactivity in the mouse cerebellum was diminished under hypoxic conditions for 5 min or direct administration of an AT1R antagonist, losartan, whereas it did not change in the zona glomerulosa of the mouse adrenal cortex even after 15 min of hypoxia. The hypoxia-induced immunostaining change of AT2R mostly resembled that of AT1R.

Materials and methods

Animals

The present animal experiment was approved by the University of Yamanashi Animal Care and Use Committee. Male 33 C57BL/6 J mice, 8 weeks old, were divided into 11 groups. The mice were anesthetized with sodium pentobarbital (100 µg/g body weight), and their cerebellar organs and adrenal glands were prepared for immunohistochemical studies by three different preparation methods and also for immunoblotting analyses (Fig. 1a).

In vivo cryotechnique (IVCT) and freeze-substitution (FS)

For the control group, IVCT was performed with an in vivo cryoapparatus (IV-II; EIKO Engineering, Hitachinaka, Ibaraki, Japan) on living mouse cerebellum under normal respiration conditions (Fig. 1b), as reported previously (Ohno et al. 2006). For the experimental hypoxia groups, IVCT was performed at 1, 5, 10 or 15 min after opening the thoracic cavity (Saitoh et al. 2009). To expose the cerebellum of anesthetized mice, a part of the cranial bone was carefully removed with a dental electric drill (Ohno et al. 2007). IVCT was performed by directly cutting the cerebellum with a cryoknife precooled in liquid nitrogen (−196 °C) (Fig. 1b) (Ohno et al. 1996), and then immediately pouring isopentane–propane (IP) cryogen (−193 °C) over it under the in vivo cryoapparatus (Fig. 1b). In another experiment with an AT1R antagonist of losartan (Li et al. 1993), the losartan solution (20 µg/ml) was directly dropped on the exposed cerebellum of anesthetized mice, and then the IP cryogen (−193 °C) was directly poured over the cerebellum at 7 min after the administration of losartan in the same way as for adrenal glands as described below.

For adrenal glands of anesthetized mice (Fig. 1c), the abdominal cavity was carefully opened, the adrenal glands on the left side were exposed, and immediately IP cryogen (−193 °C) was poured on them. Then, the frozen adrenal tissues were removed from the abdominal cavity with a dental electric drill in liquid nitrogen (−196 °C).

The frozen cerebellar and adrenal tissues were all freeze-substituted with acetone containing 2 % paraformaldehyde at −80 °C for 28 h, and then at −30, −10 and 4 °C for 2 h each and finally raised up to room temperature (RT); they were then routinely embedded in paraffin wax, as described previously (Fig. 1a) (Ohno et al. 2006).

Quick-freezing of fresh resected tissues and freeze-substitution (QF-FS)

For morphological and immunohistochemical comparison, some pieces of resected cerebellar tissues, as described in a previous paper (Ohno et al. 2006), were quickly plunged into liquid IP cryogen (−193 °C) precooled in liquid nitrogen (Fig. 1a). The time interval between resection of tissues and their quick-freezing was about 1 min. The frozen cerebellar tissues were routinely freeze-substituted and embedded in paraffin wax, as described above.

Perfusion-fixation followed by routine alcohol dehydration (PF-DH)

Other pieces of small cerebellar tissues obtained by conventional perfusion-fixation with 2 % paraformaldehyde in

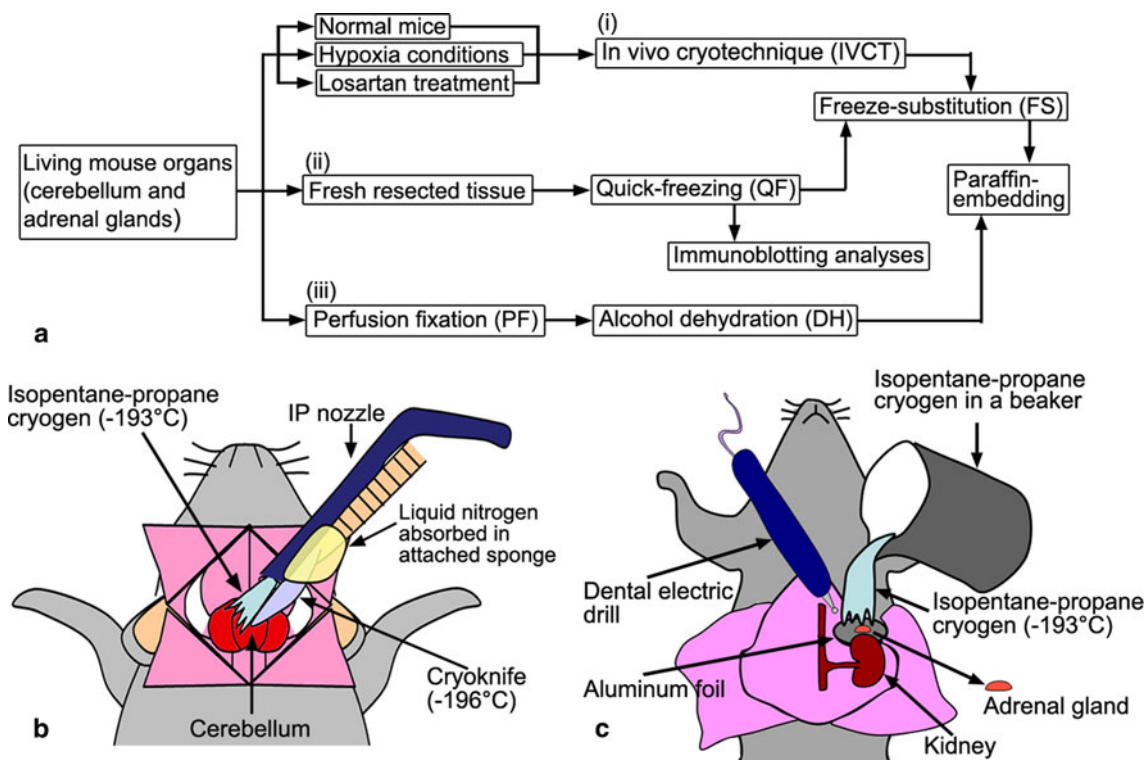


Fig. 1 **a** A flow chart of the three different preparation procedures, namely, in vivo cryotechnique with freeze-substitution (i) quick-freezing of fresh resected tissues followed by freeze-substitution (ii) and conventional perfusion fixation with alcohol dehydration (iii) for mouse organs, such as cerebellum or adrenal glands, which are finally embedded in paraffin wax. **b** A schematic drawing of the in vivo cryotechnique for an anesthetized mouse cerebellum under an in vivo cryoapparatus. It is frozen in vivo with a cryoknife and simultaneously has isopentane-propane (IP) cryogen (-193°C) poured on it.

c Another schematic drawing of a manual “in vivo cryotechnique” for an adrenal gland, which is a simple method without the in vivo cryoapparatus. An abdominal cavity of an anesthetized mouse is opened, and a tiny piece of aluminum sheet is inserted under the adrenal gland. Then, IP cryogen in a beaker is directly poured over it, which is immediately followed by plunging the whole mouse body into liquid nitrogen (-196°C). The frozen adrenal gland is removed in the liquid nitrogen using a dental electric drill, as shown in the scheme

0.1 M phosphate buffer (pH 7.4) were additionally immersed in the same fixative at 4°C overnight (Fig. 1a). Then, the fixed specimens were routinely dehydrated with a graded series of ethanol, immersed in xylene and finally embedded in paraffin wax.

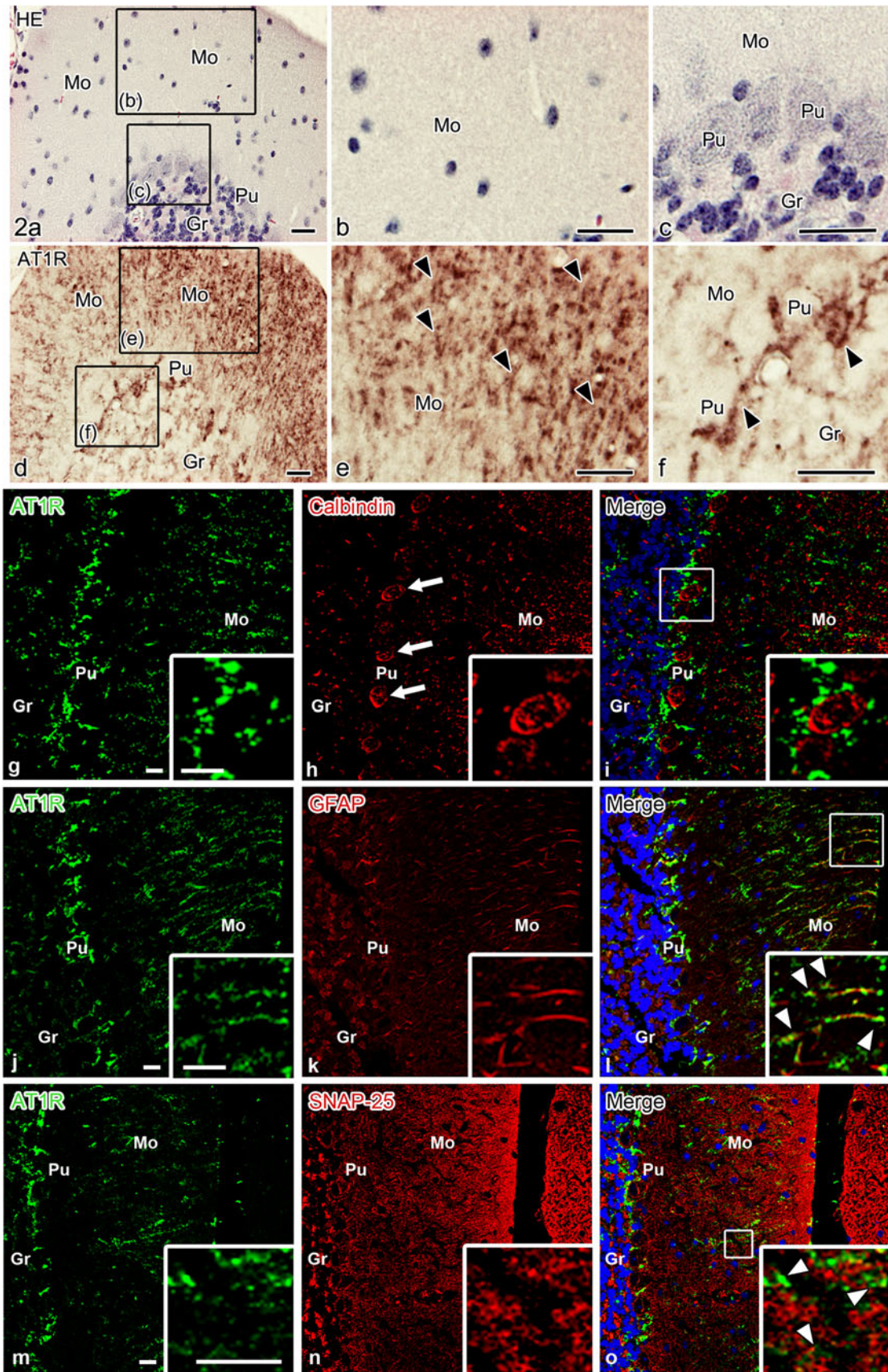
HE-staining and immunostaining for AT1R and AT2R

Paraffin sections were serially cut at $4\ \mu\text{m}$ thickness, and mounted on Matsunami Adhesive Slide (MAS)-coated glass slides (Matsunami Glass, Osaka, Japan). The sections were deparaffinized with xylene and rehydrated in a graded series of ethanol and phosphate-buffered saline (PBS). Some sections were routinely stained with hematoxylin-eosin (HE) and observed for pure morphology under a light microscope (BX-61; Olympus, Tokyo, Japan).

Other deparaffinized sections were incubated with 0.3 % hydrogen peroxide in phosphate-buffered saline (PBS; pH 7.4) at RT for 60 min. Subsequently, they were incubated with 1 % bovine serum albumin (BSA) at RT for 2 h, and then with rabbit polyclonal anti-AT1R (1/50 ADI-905-743)

or AT2R (1/50 ADI-905-746) antibody (Enzo Life Sciences, Farmingdale, NY, USA) at 4°C overnight. As described in “Results”, these antibodies are characterized by our findings: (1) the immunoreactivities of AT1R and AT2R were clearly detected in the adrenal gland, where expressions of AT receptors were well characterized (Yatabe et al. 2011), (2) the molecular weights of the target proteins detected in the western blotting were the same as those reported previously (Servant et al. 1994; Jayadev et al. 1999), (3) the target proteins in the cerebellum have the same molecular weight as those expressed in the adrenal gland. They were then incubated with biotinylated anti-rabbit IgG (1/500) antibody (Vector, Burlingame, CA, USA) at RT for 1 h, and visualized by the avidin–biotin complex–diaminobenzidine (ABC-DAB) method (ThermoSci., Rockford, IL, USA). Immunoccontrols were performed without the primary antibodies.

For double-immunofluorescence staining, sections were incubated with goat polyclonal anti-calbindin (1/1,000) antibody (Santa Cruz Biotech., Santa Cruz, CA, USA) or goat polyclonal anti-GFAP (1/50) antibody (NeuroMics



◀ **Fig. 2 a–f** Light microscopic images of HE staining (**a–c**) and immunostaining of AT1R (**d–f**) in mouse cerebellum under normal blood circulation, as prepared using IVCT-FS. **b, c** and **e, f**: Highly magnified views of rectangular areas in (**a**) and (**d**), respectively. AT1R immunostaining is detected in molecular layers (Mo), Purkinje cell layers (Pu) and granular layers (Gr) in the cerebellum (**d–f**). At higher magnification, immunostaining patterns in the molecular layer are shown as many tiny *dots* that are mostly arranged in *lines* (**e, arrowheads**), which are also seen around Purkinje cells (**f, arrowheads**). **g–o** Confocal laser scanning micrographs of double-immunofluorescence staining of AT1R with calbindin (**g–i**), GFAP (**j–l**) or SNAP-25 (**m–o**) in the mouse cerebellum, as prepared using IVCT-FS. The *green* AT1R fluorescence, appearing like *dots* lining in the molecular layers and around the Purkinje cells (**g, j, m**), does not often colocalize with calbindin (**i**) or SNAP-25 (**o, arrowheads**), but largely overlap with the *line-patterns* of GFAP (**l, arrowheads**). *Insets*: Highly magnified views of *rectangular boxed areas*. *Topro3 blue* nuclear staining. *Bars* 20 μm

Antibodies, Minneapolis, MN, USA) along with rabbit anti-AT1R or -AT2R antibody overnight. Then, they were incubated with AlexaFluor 488-conjugated donkey anti-rabbit IgG (1/200) and AlexaFluor 594-conjugated donkey anti-goat IgG (1/200) antibodies (Invitrogen, Carlsbad, CA, USA) for 2 h. They were washed in PBS, embedded in Vectashield (Vector, Burlingame, CA, USA) and routinely observed under a confocal laser scanning microscope (CLSM) (FV1000; Olympus, Tokyo, Japan). In the CLSM observation, the used objective lens was $\times 40$ with the pinhole size of 80 μm . The resolution was 0.397 $\mu\text{m}/\text{pix}$ in x - y axis, and optical thickness was 1.027 μm in z axis.

Immunoblotting analyses for AT1R and AT2R in cerebellum or adrenal gland

Mouse cerebellar tissues and adrenal glands were removed from the cranial cavity and the abdominal cavity, respectively, and cut into several small pieces with a razor blade, and then immediately plunged into isopentane cryogen precooled with dry ice. They were then homogenized with pestles and heated in Laemmli buffer (Bio-Rad, Hercules, CA, USA) at 1/50 of tissue/buffer ratio at 95 °C for 15 min. The Laemmli buffer contained 2 % SDS and 5 % β -mercaptoethanol. The homogenates were cooled on ice and centrifuged at 16,000 rpm for 5 min. The protein density of the supernatant was measured by BCA Protein Assay Kit (ThermoSci., Rockford, IL, USA). Bovine serum albumin of 100 mg was dissolved in the Laemmli buffer, and the BSA solution and the sample (dissolved in Laemmli buffer) were diluted 1:100 with DW, and the diluted BSA were further diluted sequentially at 1/2 with 1 % Laemmli buffer to draw a standard curve. And 40 μg of total protein was subjected to 5–20 % gradient gel electrophoresis (SDS-PAGE) (ATTO, Tokyo, Japan). Separated protein bands were electrotransferred to polyvinylidene fluoride membranes (Millipore, Bedford,

MA, USA), which were blocked with 5 % bovine serum albumin (Sigma) in PBS for 2 h and then immunostained with anti-AT1R (1/300) or -AT2R (1/160) antibodies at 4 °C overnight. They were then incubated with biotinylated anti-rabbit IgG (1/3,000) antibody (Vector, Burlingame, CA, USA) at RT for 2 h and finally visualized by the avidin–biotin complex–diaminobenzidine (ABC–DAB) method (ThermoSci., Rockford, IL, USA). Immunocontrols were performed without the primary antibodies.

Results

Immunostaining for AT1R was first performed in cerebellar tissues of anesthetized mice prepared using IVCT (Fig. 2). Immunoreaction products of AT1R were localized in all three layers of the mouse cerebellar cortex, including molecular, Purkinje cell and granular layers (Fig. 2a, d). In the three layers, AT1R immunoreactivity was higher in the molecular layers, and the immunostaining pattern was shown as many tiny dots lining the region from Purkinje cell layers to outer tissue areas of molecular layers (Fig. 2a, b, d, e). In the Purkinje cell layers, however, their immunostaining appeared to be localized around Purkinje cells (Fig. 2c, f). In the granular layers, less immunoreaction products were observed among granule cells, compared with those in the molecular and Purkinje cell layers (Fig. 2c, f). To investigate the immunolocalization of AT1R in the mouse cerebellum further, double-immunofluorescence staining for AT1R and calbindin, a marker of Purkinje cells, was performed in the same section (Fig. 2g–i). The calbindin was immunolocalized in large cell bodies, dendritic processes and axons of Purkinje cells in the cerebellar cortex (Fig. 2h), but the immunostaining for AT1R did not colocalize with that of calbindin (Fig. 2g–i). On the other hand, in double-immunofluorescence staining for AT1R and GFAP, a marker of Bergmann glia in both molecular and Purkinje cell layers and astrocytes in the granular layers, the immunoreaction products of AT1R largely overlapped with those of GFAP in the outer molecular layers (Fig. 2j–l). In double-immunostaining with SNAP-25, a membrane-anchored protein at the cytosolic face of pre-synaptic terminals (Sudhof and Rothman 2009), we found that the immunoreactivity of AT1R appeared to surround the dot-like SNAP-25 immunoproductions in the molecular layer, but the overlapping between AT1R and SNAP-25 was little (Fig. 2m–o).

It has already been reported that immunolocalizations of dynamic molecules in signal transduction pathways can be easily changed by conventional preparation methods (Ohno et al. 2004). To examine whether the immunostaining patterns of AT1R are consistent among the different tissue preparation methods, the immunolocalization of AT1R was

Fig. 3 Immunostaining of AT1R with the three different preparation methods, namely, IVCT-FS (a–c), QF-FS (d–f) and PF-DH (g–i). Immunoreaction products in the specimens prepared using IVCT-FS are more clearly detected in molecular layers (Mo), Purkinje cell layers (Pu) and granular layers (Gr) than those prepared using QF-FS and PF-DH. At higher magnification, immunoreaction products, recognized as *dot-patterns*, are less clear in the molecular layers using QF-FS and PF-DH (b, e, h, arrowheads), and also less clear in Purkinje cell layers with QF-FS and PF-DH (c, f, i, arrowheads). Bars 20 μ m

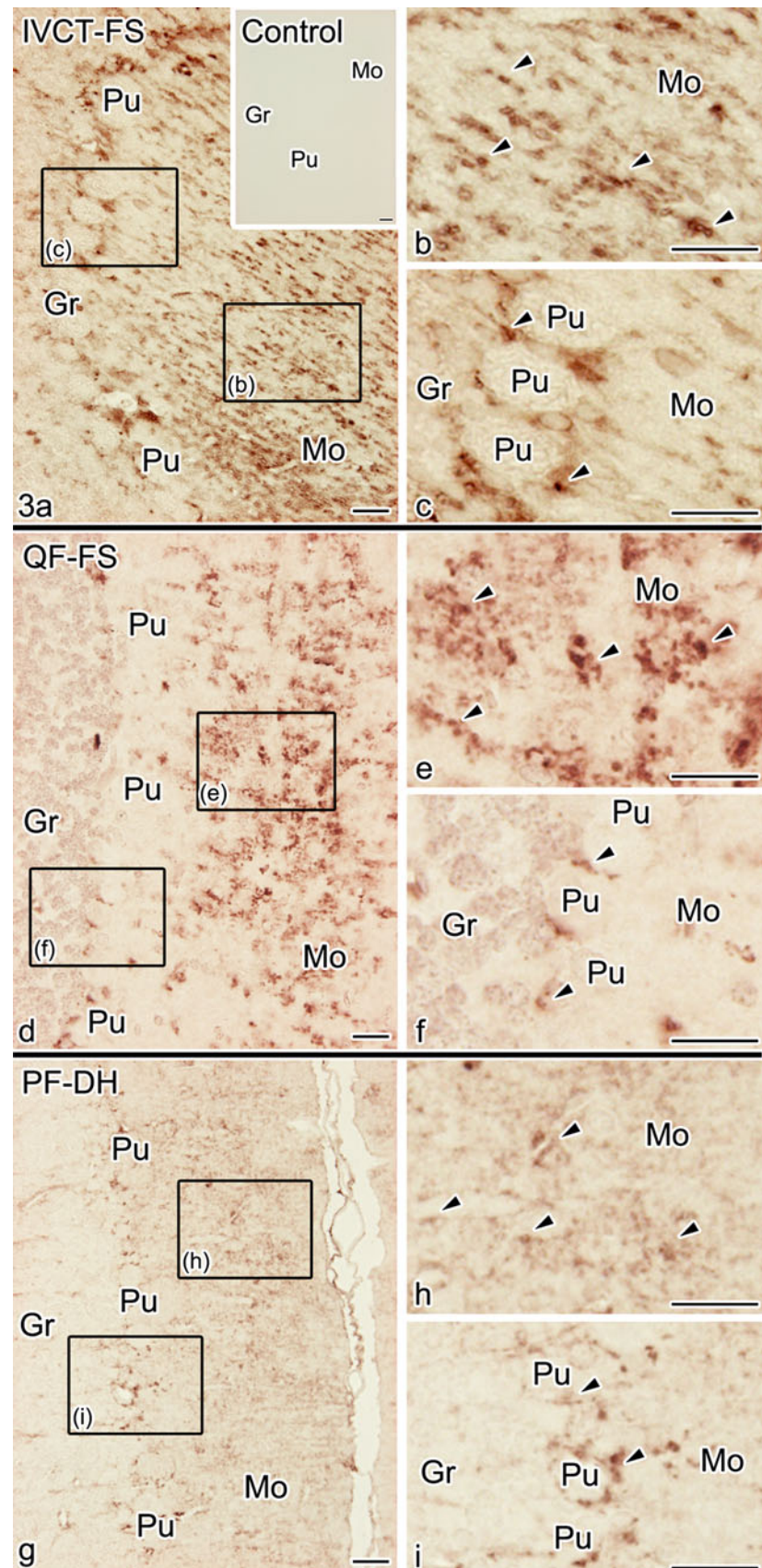


Table 1 Semi-quantitative comparison of AT1R immunoreactivity in mouse cerebellum among the three different preparation procedures, namely, IVCT-FS, QF-FS and PF-DH

Different preparation procedures	Molecular layer		Purkinje cell layer	Granular layer
	Outer	Inner		
IVCT-FS	++	+	+	+
QF-FS	+	+/-	+	+/-
PF-DH	+/-	+/-	+	-
Losartan administration with IVCT	-	+/-	+/-	+/-

In addition to administration of an antagonist, losartan. (++): strongly immunopositive, (+): moderately immunopositive, (+/-): slightly immunopositive, (-): negative

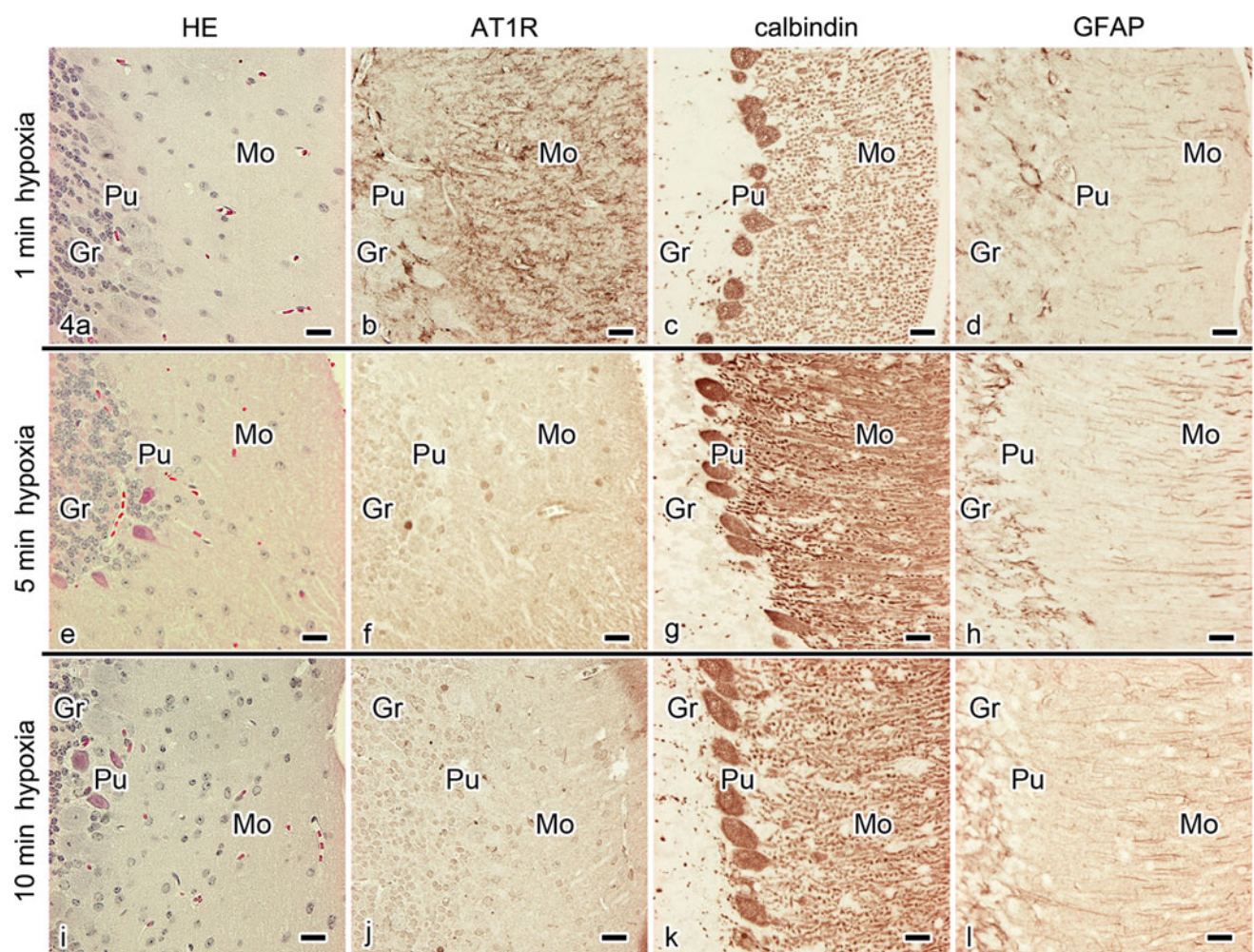


Fig. 4 Light microscopic images of HE staining (a, e, i) and immunostaining of AT1R (b, f, j), calbindin (c, g, k) and GFAP (d, h, l) under 1 (a–d), 5 (e–h) and 10 (i–l) min hypoxia in serial sections of the mouse cerebellum, as prepared using IVCT-FS. At 1 min after hypoxia, AT1R immunoreactivity is still detected, whereas its intensity is slightly decreased in comparison with those of normal mice, as shown in Figs. 2d and 3a. At 5 (f) and 10 (j) min

of hypoxia, AT1R immunoreactivity is remarkably reduced in all three layers, namely, molecular layer (Mo), Purkinje cell layer (Pu) and granular layer (Gr). Moreover, as seen by HE staining (e, i), some Purkinje cells show more eosinophilic cytoplasm at 5 and 10 min after hypoxia. By contrast, immunostaining of calbindin or GFAP does not change following hypoxia. Bars 20 μm

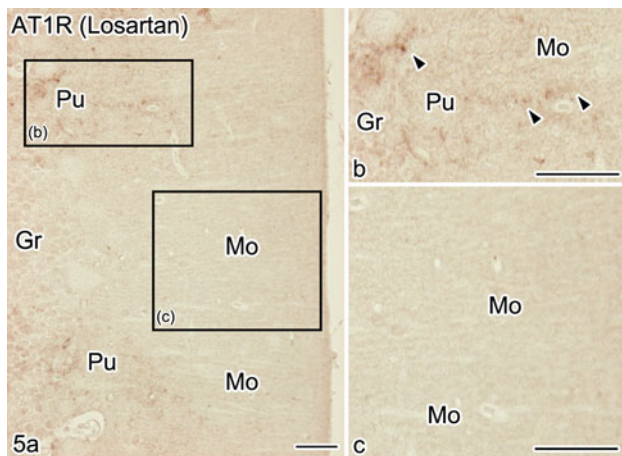


Fig. 5 Immunostaining of AT1R at 7 min after administration of an AT1R antagonist, losartan (**a**). Immunoreaction products in molecular layers (Mo), Purkinje cell layers (Pu) and granular layers (Gr) are mostly lost (**c**), but deep tissue areas still show some weaker immunoreaction (**b**, arrowheads). **b**, **c** Higher magnification of rectangular boxed areas shown in (**a**). Bars 20 μm

further examined using two other preparation methods, namely QF-FS and PF-DH (Figs. 1a, 3). The immunolocalizations of AT1R examined using QF-FS were mostly similar to those prepared using IVCT (Fig. 3a–f), and immunoreaction products appeared to be clustered or linear dot-patterns in the mouse cerebellar cortex. However, compared with the AT1R immunoreactivity detected using IVCT (Fig. 3a–c), it was more weakly detected in all three layers using QF-FS (Fig. 3d–f, Table 1). Using the conventional PF-DH (Fig. 3g–i), the AT1R immunoreactivity was less obviously detected in the three layers (Table 1).

Our previous studies demonstrated that both QF-FS and PF-DH easily caused technical artifacts of morphology because of hypoxia/ischemia inevitably induced by the conventional chemical fixation (Ohno et al. 2010). Therefore, the decreased AT1R immunoreactivity following both QF-FS and PF-DH preparations indicated that the immunostaining of AT1R was inevitably altered by hypoxic conditions. To confirm this possibility, the immunoreactivity of AT1R was examined in mouse cerebellum prepared using IVCT under different intervals of hypoxia. IVCT was similarly performed at three time points under hypoxia after opening the thoracic cavity, as shown in Fig. 1b. Following 1 min of hypoxia, the immunoreactivity of AT1R was slightly decreased, but still clearly detected in all three layers of cerebellar cortex (Fig. 4a, b). However, after 5 and 10 min of hypoxia, it was remarkably reduced and undetectable in the three layers (Fig. 4e, f, i, j). By contrast, the immunoreactivities of both calbindin (Fig. 4c, g, k) and GFAP (Fig. 4d, h, l) were mostly unchanged under such hypoxic conditions.

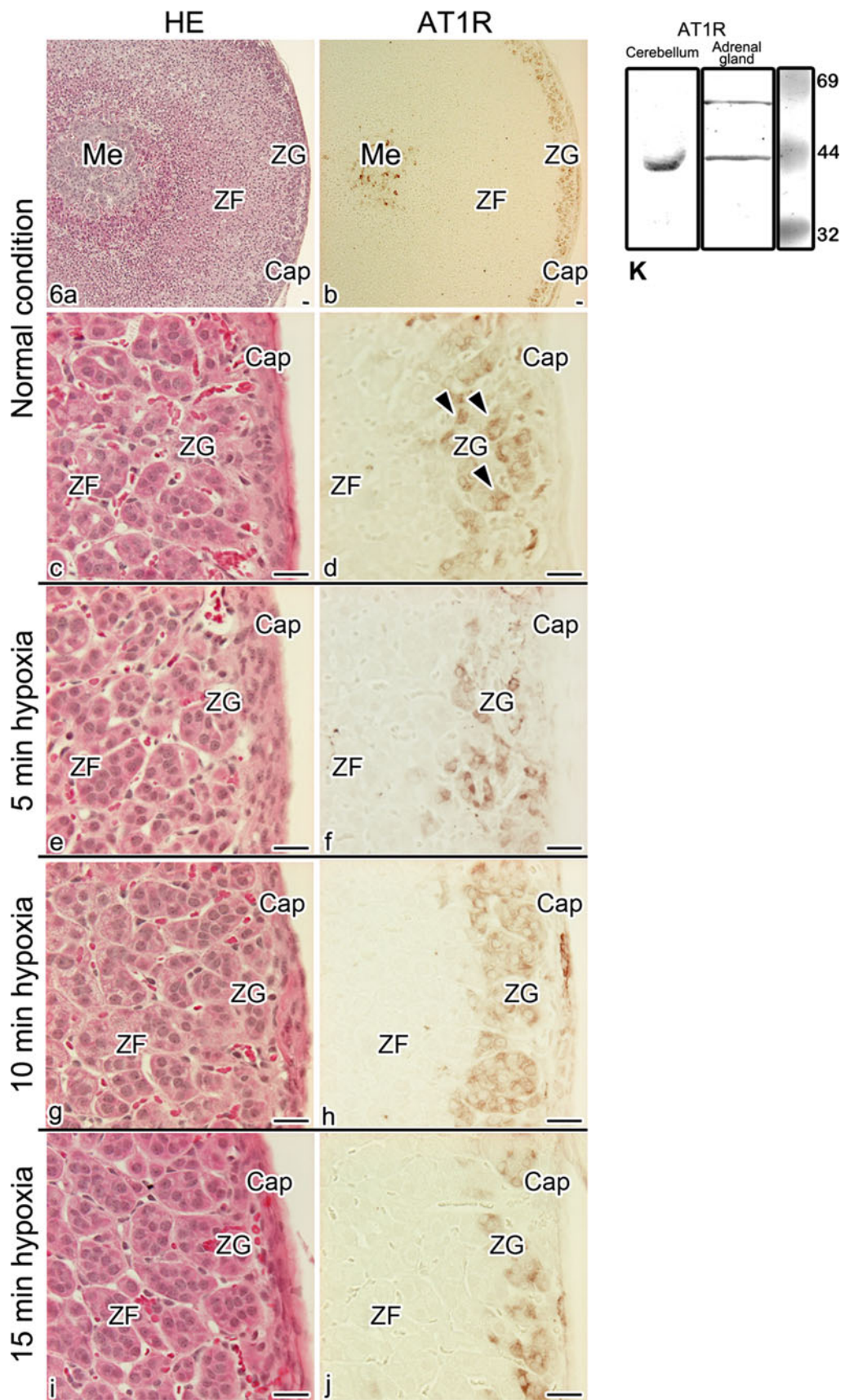
It was also reported that the binding of ligands to G-protein-coupled receptors, including AT1R, often altered

Fig. 6 a–d Light microscopic images of HE staining (**a**, **c**) and immunostaining of AT1R (**b**, **d**) in mouse adrenal glands under normal blood circulation, as prepared using IVCT-FS. **b** The AT1R antibody mostly immunostains endocrine cells in the zona glomerulosa (ZG) of the adrenal cortex and some in the medulla (Me), but not those in zona fasciculata (ZF). The cytoplasm is more clearly immunostained than the nucleus (**d**, arrowheads). **e–j** Light micrographs of HE staining (**e**, **g**, **i**) and AT1R immunostaining (**f**, **h**, **j**) under 5, 10 and 15 min hypoxia in mouse adrenal glands. Immunoreaction products are still detected up to 15 min of hypoxia (**j**). **k** By immunoblotting analyses of adrenal glands with the AT1R antibody, one more band besides the 41 kDa band in the cerebellum is shown, which corresponds to about 60 kDa. Cap capsule. Bars 20 μm

the immunoreactivities of antibodies against their extracellular amino-terminal regions (Fadhil et al. 2004; Gupta et al. 2007). We examined whether AT1R immunoreactivity was changed by blocking AT binding to AT1R using an antagonist, losartan. At 7 min after direct administration of losartan onto the exposed cerebellum, the AT1R immunoreactivity was largely reduced in mouse cerebellar cortex (Fig. 5). These findings suggest that the AT1R immunoreactivity is easily decreased by hypoxia, and hindrance of receptor activation can decrease the immunoreactivity in the mouse cerebellar cortex.

The expression and functions of the AT receptors have already been established in the zona glomerulosa of the adrenal cortex, where they are involved in the production and secretion of mineral corticoids. To examine whether hypoxic conditions also affect such immunoreactivity of AT1R in the adrenal cortex, similar immunostaining for AT1R was performed in IVCT-prepared adrenal tissues with or without hypoxia (Fig. 6). The immunoreactivities of AT1R were mainly detected in the zona glomerulosa of the adrenal cortex and slightly in the adrenal medulla under normal conditions (Fig. 6a–d), as previously reported (Frei et al. 2001). Surprisingly, the immunoreactivity of AT1R was unchanged in the zona glomerulosa under hypoxic conditions (Fig. 6e–j) and similarly detected even after 15 min of hypoxia (Fig. 6j), compared with that under normal conditions (Fig. 6d). By immunoblotting analyses (Fig. 6k), the AT1R antibody showed one band at approximately 41 kDa in both cerebellum and adrenal glands, which is compatible with the previously reported molecular weight (Jayadev et al. 1999; Rakugi et al. 1997), although an additional band was found in the adrenal glands.

We next examined the immunolocalizations of another AT receptor, AT2R, in the mouse cerebellum using an antibody against extracellular N-terminal regions of AT2R. AT2R was similarly immunolocalized in all three layers of the cerebellar cortex with the most prominent immunoreaction in outer molecular layers (Fig. 7a–c). The immunostaining pattern of AT2R appears as parallel-lined tiny



dots (Fig. 7b) and to be clustered around Purkinje cells (Fig. 7c). Double-immunofluorescence staining of AT2R with GFAP or calbindin revealed that the AT2R immunoreactivity largely overlapped with that of GFAP-immunopositive processes of Bergmann glia in the cerebellar cortex (Fig. 7g–i), but not with that of calbindin-immunopositive Purkinje cells (Fig. 7d–f). In double-immunostaining with SNAP-25, the overlapping between AT2R and SNAP-25 was minimal (Fig. 7j–l).

Next, considering the hypoxic conditions, the immunoreactivity of AT2R in the cerebellar cortex was still detected at 1 min of hypoxia (Fig. 8a), which was similar to that of AT1R (Fig. 4b), but it was remarkably reduced at 5 or 10 min of hypoxia (Fig. 8b, c). However, it was also detected in the zona glomerulosa of adrenal glands under normal conditions, and did not change even at 15 min of hypoxia (Fig. 8e, f), similar to the findings for AT1R (Fig. 6). By immunoblotting analyses (Fig. 8g), AT2R antibody showed one band at approximately 35 kDa in both cerebellum and adrenal glands, although a few additional bands were also found in the adrenal cortex.

Discussion

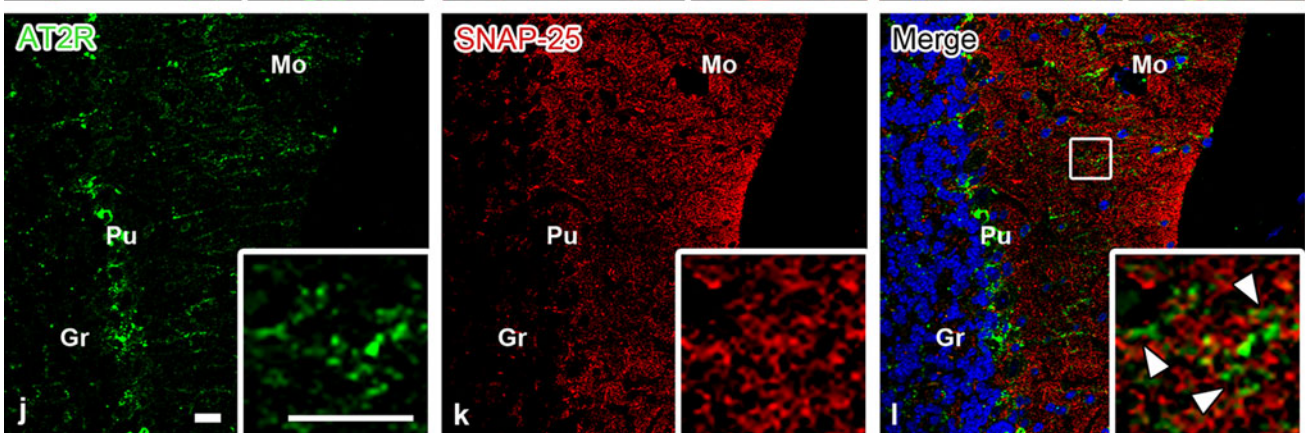
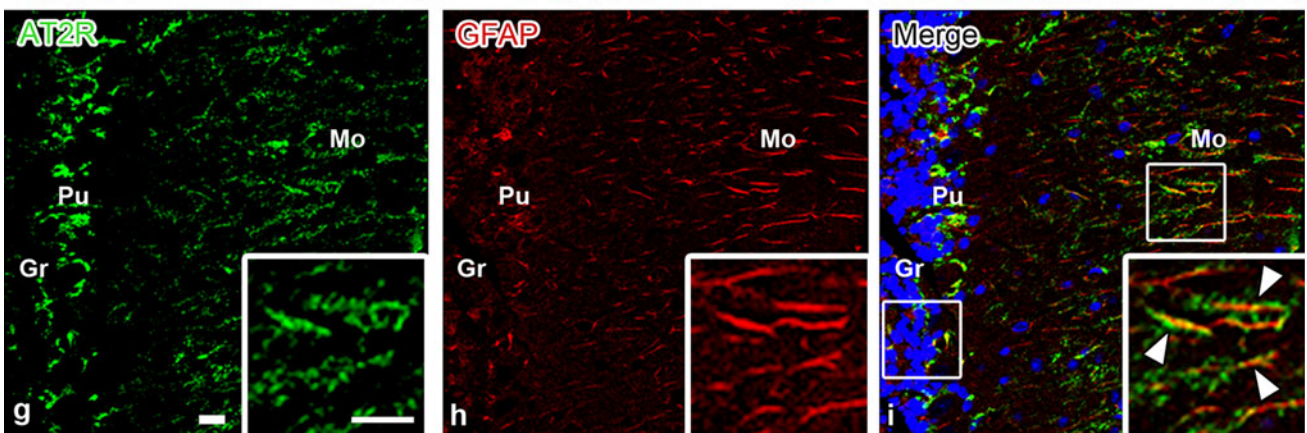
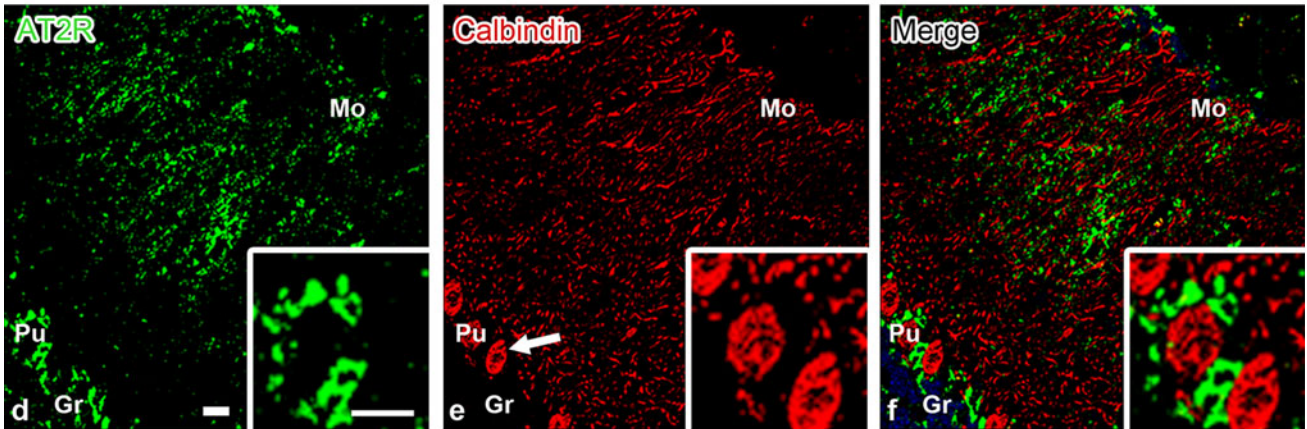
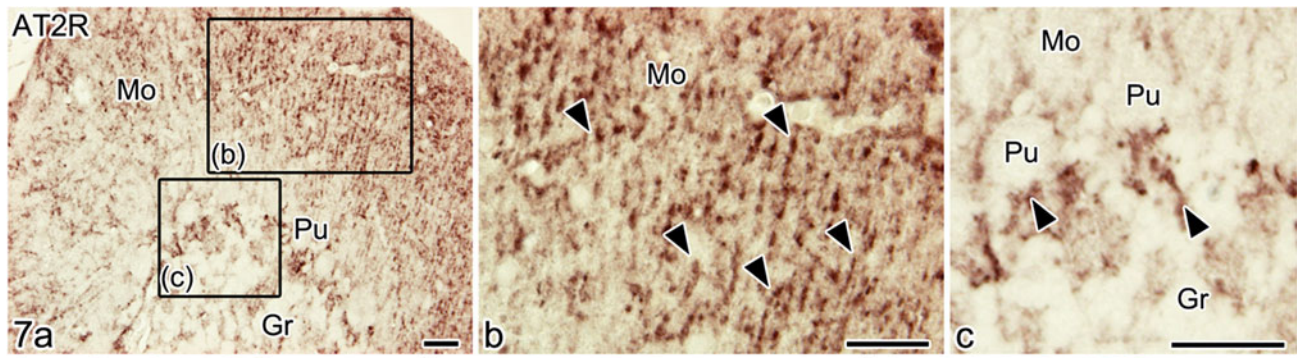
With IVCT-FS, several technical problems in clarifying the native tissue morphology and the precise immunolocalizations of signal molecules or receptors were avoidable, including tissue shrinkage and the translocation of soluble proteins caused by chemical fixation and alcohol dehydration (Terada et al. 2006; Saitoh et al. 2009; Ohno et al. 2010). The meshwork-like structures induced by the tiny ice crystal formation probably facilitate effective penetration of antibodies during immunohistochemical steps, resulting in better formation of antigen–antibody complexes (Ohno et al. 2005). Moreover, freeze-substitution (FS) fixation has an additional benefit of avoiding antigen-retrieval treatments. Therefore, we were able to obtain clearer immunolocalizations of AT1R and AT2R in the mouse cerebellum and adrenal gland with IVCT-FS compared with QF-FS and PF-DH.

In the present study, both AT1R and AT2R were immunolocalized in the molecular, Purkinje cell and granular layers of mouse cerebellum, and also zona glomerulosa and medulla of the adrenal gland. Functions of AT1R and AT2R were well characterized in the zona glomerulosa and adrenal medulla (Yatabe et al. 2011). Our findings are consistent with previous reports, showing that AT receptors were located in the cerebellar cortex (Johren et al. 1998;

Fig. 7 Immunostaining of AT2R (**a, b, c**) in mouse cerebellum under normal blood circulation, as prepared using IVCT-FS. **b, c**: Highly magnified views of *rectangular boxed* areas in (**a**). Immunoreaction products are detected in molecular layers (Mo), Purkinje cell layers (Pu) and granular layers (Gr) in the cerebellum. At higher magnification (**b, c**), immunostaining patterns in the molecular layers are shown as tiny *dots* mostly arranged in *lines* (**b, arrowheads**), which are also seen around Purkinje cells (**c, arrowheads**). **d–l** Confocal laser scanning micrographs showing double-immunofluorescence staining of AT2R (*green*) with calbindin (**d–f, red**), GFAP (**g–i, red**) and SNAP-25 (**j–l, red**) in mouse cerebellum. The AT2R immunoreactivity shows the similar immunoreaction *dots lining* in the molecular layers and around Purkinje cells, and overlapped with fascicular GFAP immunostaining (**i, arrowheads**), but not with calbindin (**f**) or SNAP-25 (**l, arrowheads**). *Insets*: Highly magnified views of *rectangular boxed* areas. *Topro 3 blue* nuclear staining. *Bars* 20 μ m

Arce et al. 2001). Although some studies reported immunolocalizations of the AT receptors in some neurons including Purkinje cells (Allen et al. 1998), other recent studies also reported their expression in glial cells, including Müller cells of rodent retina and astrocytes in rat cerebellar white matter (Fogarty and Matute 2001; Fletcher et al. 2010). Moreover, in pathological tissues of axonal injury in the outer molecular layer of dentate gyrus, AT1R immunoreactivity has been found in astrocytes (Fuchtbauer et al. 2011). The overlapping of AT receptor immunoreactivity with GFAP supports the concept that the AT receptors are expressed in some astrocytes as well as Bergmann glia of mouse cerebellum, which are specialized astrocytes in the cerebellar cortex. However, further studies are necessary to reveal precise distribution of AT receptors at the ultrastructural level, and the mechanism regulating the localizations of AT receptor immunoreactivities in the cerebellar cortex.

It is also interesting that the immunoreactivity of AT receptors became rarely detectable in the mouse cerebellum following hypoxia, but did not change even after 15 min of hypoxia in the zona glomerulosa of mouse adrenal gland (Table 2). The antibodies used in this study are raised against the extracellular N-terminal regions of the AT receptors (Gupta et al. 2007), which undergo conformational changes upon receptor activation (Lecat et al. 2002). One possibility for the reduced immunoreactivity is that molecular structures of the AT receptors, AT1R and AT2R, bound to ligands can be effectively retained using IVCT, and it could capture dynamic detachment of AT ligands from the AT receptors and conformational alteration of the receptors from activated to non-activated states, as reported previously for rhodopsin (Terada et al.



2006). This concept is supported by the finding that administration of an antagonist, losartan, largely eliminated AT1R immunoreactivity in mouse cerebellar cortex. Administration of the AT1R antagonist has already been reported to lead to a protective effect against ischemia in rat retina and cerebrum (Liu et al. 2008; Fukuda et al. 2010). Although further studies are necessary to confirm that the immunoreactivity changes observed in this study are attributable exclusively to alterations of ligand binding and/or receptor activities, our results suggest that the local angiotensin system is one of the signal transduction pathways in the mouse cerebellum under physiological conditions, and both AT receptors are involved in rapid adaptation against hypoxic injury.

The different responses of cerebellum and adrenal glands to hypoxia might be attributable to their different glycosylation states. Both AT1R and AT2R in different animal organs have various molecular weights ranging from 31 to 200 kDa (Servant et al. 1994; Jayadev et al. 1999; Frei et al. 2001; Fogarty and Matute 2001; Harada et al. 2010). In previous reports, mutations of glycosylation sites in AT1R and endoglycosidase digestion of AT2R demonstrated that different molecular weights of the AT

receptors are largely due to various degrees of glycosylation (Servant et al. 1994; Jayadev et al. 1999). Unglycosylated AT1R and AT2R have reduced molecular sizes, namely, 41 and 31 kDa, consistent with the present data. The different molecular weights of AT receptors in cerebellum and adrenal glands support the notion in previous reports that increased or decreased glycosylation in the two different mouse organs. The AT-binding affinity was significantly decreased by the addition of an N-glycosylation sequon to the AT1R molecule (Lanctot et al. 2005). Glycosylation of AT1R and AT2R may contribute to AT ligand affinity as well as their molecular stability and intracellular trafficking or targeting. A non-glycosylated luteinizing hormone receptor has no binding activities against luteinizing hormone because of much lower molecular stability (Zhang et al. 1995). In addition, glycosylation of Nkp30 receptor could provide a switch to control ligand-binding properties of the receptor and consequently regulate the cytotoxicity function of natural killer cells (Hartmann et al. 2012). Collectively, our present findings also indicate that down-regulated functions of the AT receptors under hypoxia depend on their different glycosylation levels in the cerebellum and adrenal glands

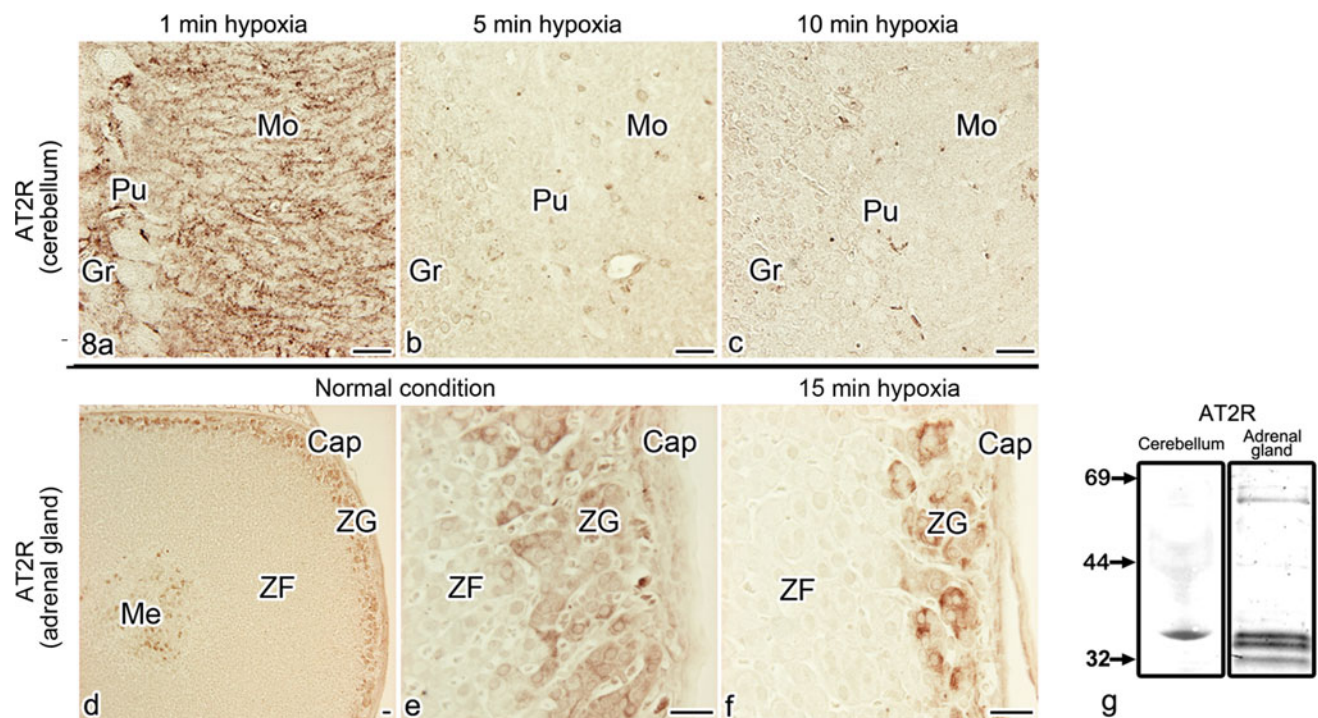


Fig. 8 Immunostaining of AT2R under hypoxic conditions in mouse cerebellum and adrenal glands, as prepared using IVCT-FS. **a–c** In the cerebellum, at 1 min after hypoxia (**a**), immunoreaction products are still detected as dot-patterns, but their immunostaining intensities are slightly decreased in comparison with those of normal mice, as shown in Fig. 7a–c. After 5 and 10 min of hypoxia (**b**, **c**), they are remarkably reduced in all three molecular (Mo), Purkinje cell (Pu) and granular layers (Gr). **d–f** In the adrenal glands, however, the

immunoreaction products, which are detected in adrenal medulla (Me) and zona glomerulosa (ZG) in adrenal cortex but not in zona fasciculata (ZF), are still detected up to 15 min hypoxia (**f**). (**g**) By immunoblotting analyses, only a 35 kDa band is found in the mouse cerebellum, but a few additional bands including a 60 kDa band and two bands smaller than 35 kDa are seen in the adrenal glands. Cap capsule. Bars 20 μ m

Table 2 Semi-quantitative comparison of AT1R and AT2R immunoreactivities in mouse cerebellum and adrenal gland under hypoxia. Angiotensin II receptor type 1 and type 2 (AT1R and AT2R)

Cerebellum	Cerebellum			Adrenal gland		
	Molecular layer		Purkinje cell layer	Granular layer	Zona glomerulosa	
	Outer	Inner				
Normal condition	++	+	+	+	Normal condition	+
Hypoxia 1 min	+	+	+	+	Hypoxia 5 min	+
Hypoxia 5 min	–	–	–	–	Hypoxia 10 min	+
Hypoxia 10 min	–	–	–	–	Hypoxia 15 min	+

After 5 and 10 min of hypoxia, the immunoreactivities are remarkably reduced in the cerebellum, but still detected even after 15 min of hypoxia in the adrenal glands. (++): strongly immunopositive, (+): immunopositive, (–): negative

by their post-translational modification, resulting in various levels of ligand affinity and molecular stability.

References

- Allen AM, Moeller I, Jenkins TA, Zhuo J, Aldred GP, Chai SY, Mendelsohn FA (1998) Angiotensin receptors in the nervous system. *Brain Res Bull* 47:17–28
- Arce ME, Sanchez S, Seltzer A, Ciuffo GM (2001) Autoradiographic localization of angiotensin II receptors in developing rat cerebellum and brainstem. *Regul Peptides* 99:53–60
- Arce ME, Sanchez SI, Aguilera FL, Seguin LR, Seltzer AM, Ciuffo GM (2011) Purkinje cells express angiotensin II AT2 receptors at different developmental stages. *Neuropeptides* 45:69–76
- Basso N, Terragno NA (2001) History about the discovery of the rennin-angiotensin system. *Hypertension* 38:1246–1249
- Changaris DG, Severs WB, Keil LC (1978) Localization of angiotensin in rat brain. *J Histochem Cytochem* 26:593–607
- Cote F, Do TH, Laflamme L, Gallo JM, Gallo-Payet N (1999) Activation of the AT2 receptor of angiotensin II induces neurite outgrowth and cell migration in microexplant cultures of the cerebellum. *J Biol Chem* 274:31686–31692
- Fadhil I, Schmidt R, Walpole C, Carpenter KA (2004) Exploring deltorphin II binding to the third extracellular loop of the delta-opioid receptor. *J Biol Chem* 279:21069–21077
- Fletcher EL, Phipps JA, Ward MM, Vessey KA, Wilkinson-Berka JL (2010) The renin-angiotensin system in retinal health and disease: its influence on neurons, glia and the vasculature. *Prog Retin Eye Res* 29:284–311
- Fogarty DJ, Matute C (2001) Angiotensin receptor-like immunoreactivity in adult brain white matter astrocytes and oligodendrocytes. *Glia* 35:131–146
- Frei N, Weissenberger J, Beck-Sickinger AG, Höfliger M, Weis J, Imboden H (2001) Immunocytochemical localization of angiotensin II receptor subtypes and angiotensin II with monoclonal antibodies in the rat adrenal gland. *Regul Peptides* 101:149–155
- Fuchtbauer L, Groth-Rasmussen M, Holm TH, Lobner M, Toft-Hansen H, Khoroshii R, Owens T (2011) Angiotensin II type 1 receptor (AT1) signaling in astrocytes regulates synaptic degeneration-induced leukocyte entry to the central nervous system. *Brain Behav Immun* 25:897–904
- Fukuda K, Hirooka K, Mizote M, Nakamura T, Itano T, Shiraga F (2010) Neuroprotection against retinal ischemia-reperfusion injury by blocking the angiotensin II type 1 receptor. *Invest Ophthalmol Vis Sci* 51:3629–3638
- Gasparo MD, Catt KJ, Inagami T, Wright JW, Unger T (2000) International union of pharmacology. XXIII. The angiotensin II receptors. *Pharmacol* 52:415–472
- Gupta A, Decaillot FM, Gomes I, Tkalych O, Heimann AS, Ferro ES (2007) Conformation state-sensitive antibodies to G-protein-coupled receptors. *J Biol Chem* 282:5116–5124
- Harada K, Matsuoka H, Fujimoto N, Endo Y, Hasegawa Y, Matsuo A, Kikuchi Y, Matsumoto T, Inoue M (2010) Localization of type-2 angiotensin II receptor in adrenal gland. *J Histochem Cytochem* 58:585–593
- Hartmann J, Tran TV, Kaudeer J, Oberle K, Herrmann J, Quagliano I, Abel T, Cohnen A, Gatterdam V, Jacobs A, Wollscheid B, Tampe R, Watzl C, Diefenbach A, Koch J (2012) The stalk domain and the glycosylation status of the activating natural killer cell receptor Nkp30 are important for ligand binding. *J Biol Chem* 287:31527–31529
- Jayadev S, Smith RD, Jagadeesh G, Baukal AJ, Hunyady L, Catt KJ (1999) N-linked glycosylation is required for optimal AT_{1a} angiotensin receptor expression in COS-7 cells. *Endocrinol* 140:2010–2017
- Johren O, Hauser W, Saavedra JM (1998) Chemical lesion of the inferior olive reduces [¹²⁵I] sarcosine-angiotensin II binding to AT2 receptors in the cerebellar cortex of young rats. *Brain Res* 793:176–186
- Lancot PM, Leclerc PC, Clement M, Auger-Messier M, Escher E, Leduc R, Guillemette G (2005) Importance of n-glycosylation positioning for cell-surface expression, targeting, affinity and quality control of the human AT1 receptor. *Biochem J* 390:367–376
- Lecat S, Bucher B, Mely Y, Galzi J (2002) Mutations in the extracellular amino-terminal domain of the NK2 neurokinin receptor abolish cAMP signaling but preserve intracellular calcium responses. *J Biol Chem* 277:42034–42048
- Li Z, Bains JS, Ferguson AV (1993) Functional evidence that the angiotensin antagonist losartan crosses the blood–brain barrier in the rat. *Brain Res Bull* 30:33–39
- Liu H, Kitazato KT, Uno M, Yagi K, Kanematsu Y, Tamura T, Tada Y, Kinouchi T, Nagahiro S (2008) Protective mechanisms of the angiotensin II type 1 receptor blocker candesartan against cerebral ischemia: in vivo and in vitro studies. *J Hypertens* 26:1435–1445
- Ohno S, Terada N, Fujii Y, Ueda H, Takayama I (1996) Dynamic structure of glomerular capillary loop as revealed by an “in vivo cryotechnique”. *Virchows Arch* 427:519–527
- Ohno N, Terada N, Fujii Y, Baba T, Ohno S (2004) “in vivo cryotechnique” for paradigm shift to “living morphology” of animal organs. *Biomed Rev* 15:1–19
- Ohno N, Terada N, Murata S, Katoh R, Ohno S (2005) Application of cryotechniques with freeze-substitution for the immunohistochemical

- demonstration of intranuclear pCREB and chromosome territory. *J Histochem Cytochem* 53:55–62
- Ohno N, Terada N, Ohno S (2006) Histochemical analyses of living mouse liver under different hemodynamic conditions by “in vivo cryotechnique”. *Histochem Cell Biol* 126:389–398
- Ohno N, Terada N, Saitoh S, Ohno S (2007) Extracellular space in mouse cerebellar cortex revealed by “in vivo cryotechnique”. *J Comp Neurol* 505:292–301
- Ohno S, Terada N, Ohno N, Saitoh S, Saitoh Y, Fujii Y (2010) Significance of ‘in vivo cryotechnique’ for morphofunctional analyses of living animal organs. *J Electron Microsc* 59:395–408
- Phillips MI, Shen L, Richards EM, Raizada MK (1993) Immunohistochemical mapping of angiotensin AT1 receptors in the brain. *Regul Peptide* 44:95–107
- Rakugi H, Okamura A, Kamide K, Ohishi M, Sasamura H, Morishita R (1997) Recognition of tissue- and subtype-specific modulation of angiotensin II receptors using antibodies against AT1 and AT2 receptors. *Hypertens Res* 20:51–55
- Reagan LP, Flanagan-Cato LM, Yee DK, Ma LY, Sakai RR, Fluharty SJ (1994) Immunohistochemical mapping of angiotensin type 2 (AT2) receptors in rat brain. *Brain Res* 662:45–59
- Saavedra JM (1992) Brain and pituitary angiotensin. *Endocrinol* 13:329–380
- Saitoh S, Terada N, Ohno N, Saitoh Y, Soleimani M, Ohno S (2009) Immunolocalization of phospho-Arg-directed protein kinase-substrate in hypoxic kidneys using in vivo cryotechnique. *Med Mol Morphol* 42:24–31
- Servant G, Dudley DT, Escher E, Guillemette G (1994) The marked disparity between the sizes of angiotensin type 2 receptors from different tissues is related to different degrees of N-glycosylation. *Mol Pharmacol* 45:1112–1118
- Sudhof TC, Rothman JE (2009) Membrane fusion: grappling with SNARE and SM proteins. *Science* 323:474–477
- Terada N, Ohno N, Ohguro H, Li Z, Ohno S (2006) Immunohistochemical detection of phosphorylated rhodopsin in light-exposed retina of living mouse with in vivo cryotechnique. *J Histochem Cytochem* 54:479–486
- Yatabe J, Yoneda M, Yatabe MS, Watanabe T, Felder RA, Jose PA, Sanada H (2011) Angiotensin III stimulates aldosterone secretion from adrenal gland partially via angiotensin II type 2 receptor but not angiotensin II type 1 receptor. *Endocrinology* 152:1582–1588
- Zhang R, Cai HQ, Fatima N, Buczko E, Dufau ML (1995) Functional glycosylation sites of the rat luteinizing hormone receptor required for ligand binding. *J Biol Chem* 270:21722–21728